

Analytical Methods

Accepted Manuscript



This is an *Accepted Manuscript*, which has been through the Royal Society of Chemistry peer review process and has been accepted for publication.

Accepted Manuscripts are published online shortly after acceptance, before technical editing, formatting and proof reading. Using this free service, authors can make their results available to the community, in citable form, before we publish the edited article. We will replace this *Accepted Manuscript* with the edited and formatted *Advance Article* as soon as it is available.

You can find more information about *Accepted Manuscripts* in the [Information for Authors](#).

Please note that technical editing may introduce minor changes to the text and/or graphics, which may alter content. The journal's standard [Terms & Conditions](#) and the [Ethical guidelines](#) still apply. In no event shall the Royal Society of Chemistry be held responsible for any errors or omissions in this *Accepted Manuscript* or any consequences arising from the use of any information it contains.

COMMUNICATION

Efficient ratiometric fluorescence probe based on dual-emission fluorescence silica nanoparticle for visual determination of Hg^{2+}

Cite this: DOI: 10.1039/x0xx00000x

Jing Wang,^a Meng Ma,^b Rongbin Huang,^a Ligeng Wang,^a Aimin Chen^{*a} and Jun Hu^{*a}

Received 00th January 2012,

Accepted 00th January 2012

DOI: 10.1039/x0xx00000x

www.rsc.org/

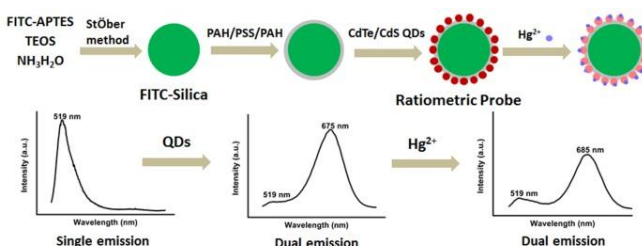
We herein designed a ratiometric fluorescence probe through hybridizing fluorescein isothiocyanate-doped silica nanoparticles with CdTe/CdS quantum dots and demonstrated its efficiency for visual detection of Hg^{2+} . The color of the solution gradually turned from red to green along with the increase of Hg^{2+} concentration.

Mercury, is considered highly toxic and widespread pollutant, and it exists in a variety of different forms (metallic, ionic, and as a part of organic salts and complexes). Mercuric ion (Hg^{2+}), as one of the most stable inorganic forms of mercury, can accumulate in organisms and interact with the thiol groups in protein to cause serious threat to human health.¹ Along with the widespread use of mercury in industry, the mercury contamination (especially Hg^{2+}) of the natural environment has attracted more and more attention. Thus, the development of rapid, sensitive and selective methods for the reliable detecting of Hg^{2+} is highly demanded and of great significance.

Thus far, various efficient and reproducible methods, including atomic absorption/fluorescence spectrometry,^{2,6} high-performance liquid chromatography,⁷ surface enhanced Raman scattering,⁸ inductively coupled plasma mass spectroscopy,⁹ circular dichroism spectra¹⁰ and voltammetric,¹¹ have been developed for the determination of Hg^{2+} . Unfortunately, those methods are usually complicated, time-consuming, and costly. In contrast, fluorescent chemodosimeters have become a powerful tool for sensing trace amounts of Hg^{2+} owing to their simplicity, high sensitivity, and short responsive time.¹²⁻¹⁸ However, most of the present chemosensors respond to Hg^{2+} by decreasing or increasing the fluorescence intensity, this single intensity-based sensing is frequently compromised by some other factors, such as the probe concentration, instrumental efficiency, and environmental effects in complex real samples. On the contrary, methods based on ratiometric fluorescence could eliminate most of the ambiguities by self-calibration of two or more different emission bands.¹⁹⁻²¹ Besides,

the signal variation of the ratiometric fluorescence probe was easier to be distinguished by the naked eyes.²²⁻²⁴

Currently, ratiometric fluorescence detection were mainly based upon dual-emission fluorescence nanoparticles, which were readily obtained by combining two different fluorophores in one nanoparticle, one fluorophore as reference and another as a signal report unit.^{25, 26} The key point for the integration of two different fluorophores was how to preserve their own emission properties during the complicated building-up process. Silica, a versatile and biocompatible material for coating layers on nano-objects, has been widely used for encapsulating various fluorescence components together and fabricating multicolor fluorescence nanoparticles.^{25, 27} To date, dyes and quantum dots (QDs)-based dual-emission silica nanoparticles have gained significant attention and developed as ratiometric fluorescence probes for metallic ion or small molecule sensing.²⁸⁻³² It was worth mentioning that although the fluorescence signal in silica core was superior, the emission properties of the response fluorophore on the surface of the silica tended to suffer a great destruction due to photobleaching²⁸ or covalent linking with a 1-ethyl-3-(3-dimethylaminopropyl) carbodiimide (EDC) coupling scheme.²⁹⁻³¹



Scheme 1 Schematic illustration of the preparation of the ratiometric probe and its detection principle for Hg^{2+}

With these insights, here we presented a simple method to prepare dual-emission silica nanoparticles for ratiometric fluorescence detection of Hg^{2+} . As illustrated in Scheme 1, fluorescein

(FITC)-doped silica nanoparticles were first synthesized using a modified Stöber method.³³ Then, a three-layer polyelectrolyte film, consisting of poly(sodium 4-styrene-sulfonate) (PSS) layer sandwiched between two layers of poly(allyamine) hydrochloride (PAH) was deposited on the surface of FITC-doped silica nanoparticles. Finally, the negatively charged N-Acetyl-L-cysteine (NAC)-capped CdTe/CdS QDs were chemisorbed on the nanoparticles through electrostatic interaction.³⁴ Notably, the resultant nanoprobe constructed by this method has several features that make it particularly attractive of Hg^{2+} : (1) the silica nanoparticles protected the reference dye (FITC) from being directly exposed to the environmental oxygen, and thus greatly enhanced the photostability of the entrapped dye;³³ (2) the response CdTe/CdS QDs were directly chemisorbed on the surface of nanoparticles, which effectively decreased the loss of fluorescence *via* covalent linking with an EDC coupling strategy;³⁴ (3) the NAC molecules which served as a strong chelating reagent for Hg^{2+} , making the rapid and selective detection of Hg^{2+} possible.^{12, 17} (4) In the presence of different amounts of Hg^{2+} , the nanoprobe displayed continuous color changes from red to green due to the quenching of the red fluorescence of QDs, which can be clearly observed by the naked eye. The experimental conditions, selectivity and sensitivity of this ratiometric fluorescence nanosensor to Hg^{2+} were carefully studied. The feasibility of the dual-emission silica nanoparticles for Hg^{2+} determination in real water samples was also investigated.

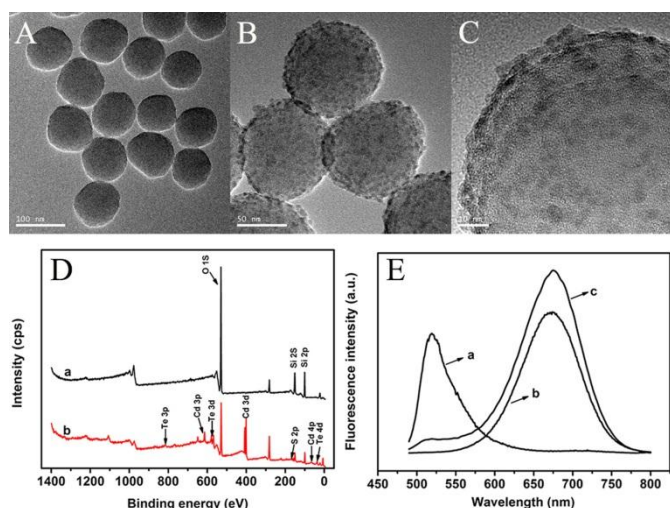


Fig. 1 (A) Typical TEM images of the as-synthesized FITC-doped silica nanoparticles and (B) dual-emission silica nanoparticles. (C) HRTEM images of dual-emission silica nanoparticles. (D) XPS spectra of FITC-doped silica nanoparticles (curve a) and dual-emission silica nanoparticles (curve b). (E) Fluorescence spectra of FITC-doped silica nanoparticles (curve a), CdTe/CdS QDs (curve b), and dual-emission silica nanoparticles (curve c).

The architecture and optical properties of the ratiometric probe were studied in detail. Typical transmission electron microscopy (TEM) images showed that the obtained FITC-doped silica cores, with an average diameter of 98 nm, were nearly spherical and smooth (Fig. 1A). The change in zeta potential effectively indicated that PAH/PSS/PAH layers were successfully deposited on the cores step by step (Fig. S1). After the chemisorption of negatively charged NAC-capped CdTe/CdS QDs (Fig. S2), the hybrid probe surfaces were

comparatively rough (Fig. 1B). High-resolution transmission electron microscopy (HRTEM) images displayed numerous, individual, dark “QD islands” on the carrier silica cores (Fig. 1C), which indicated the QDs were distributed homogeneously on the silica core surfaces. The X-ray photoelectron spectroscopy (XPS) and fluorescence spectra of the ratiometric probe further confirmed the assembly of CdTe/CdS QDs on the silica core surfaces. Compared with the spectrum of the FITC-doped silica nanoparticles (Fig. 1D, curve a), the spectrum of dual-emission silica nanoparticles (Fig. 1D, curve b) shows several new peaks at 614.5, 568.6, 401.2, 164.6 and 36.5 eV, which correspond to Cd3p_{3/2}, Te3d₅, Cd3d₅, S2p and Te4d, respectively. The amplified XPS from 200 to 0 eV was shown in Fig. S3. Meanwhile, the fluorescence spectrum (Fig. 1E) of the ratiometric probe (curve c) presents two peaks characteristic of the FITC-doped silica cores (curve a) and CdTe/CdS QDs (curve b), respectively. The red-shift of the fluorescence peak for the probe may be attributed to interparticle plasmon coupling caused by nanoparticle clusters.

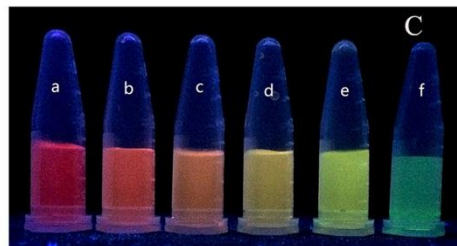
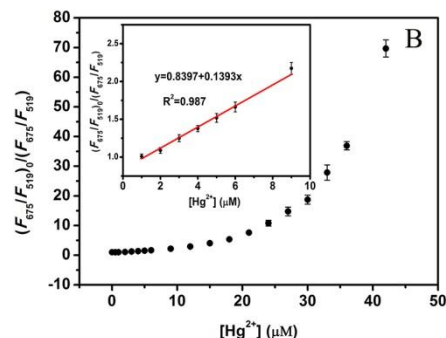
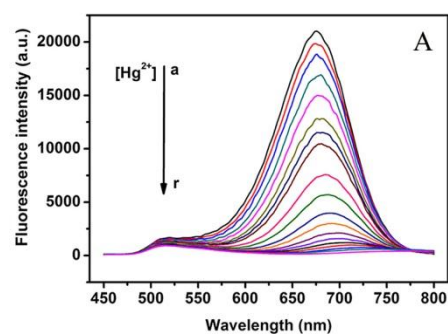


Fig. 2 (A) Fluorescence spectra ($\lambda_{\text{ex}}=365$ nm) of the ratiometric fluorescence probe upon the exposure to different concentrations of Hg^{2+} . The concentration of Hg^{2+} from the top to the bottom (a-r): 0, 0.5, 1, 2, 3, 4, 5, 6, 9, 12, 15, 18, 21, 24, 27, 30, 36, 42 μM , respectively. The final concentration of the ratiometric probe was 0.25 mg mL^{-1} . (B) Plot of fluorescence intensity ratio of $(F_{675}/F_{519})_0/(F_{675}/F_{519})$ versus the concentration of Hg^{2+} . $(F_{675}/F_{519})_0$ and (F_{675}/F_{519}) were the ratio of the fluorescence intensity of the ratiometric probe in the absence and presence of different concentrations of Hg^{2+} , respectively. Inset: Linear fitting curve of $(F_{675}/F_{519})_0/(F_{675}/F_{519})$ versus a different concentration of

Hg²⁺. (C) The fluorescence photos were taken under a UV lamp at excitation wavelength of 365 nm. The concentrations of Hg²⁺ from left to right (a-f) are 0, 2, 4, 9, 15, 21 μM, respectively.

For the dual-emission hybrid nanoparticles to be used as a ratiometric probe, photostability was an important factor to be investigated. After consecutive illuminations at 365 nm, the relative fluorescence intensity ratio (F_{675}/F_{519}) exhibited no apparent change with 120 min, implying the long-term photostability of the probe in aqueous solution (Fig. S4). In addition, we found the fluorescence intensity of each peak (675 and 519 nm) also has no significant change, which indicated the outstanding colloidal stability of the hybrid nanoparticles. The influence of pH (from 4.0 to 10.0) on the fluorescence intensity ratio of the ratiometric probe in the absence and presence of Hg²⁺ were also examined (Fig. S5). The results suggested that the pH value was a prominent factor for the determination of Hg²⁺ and the optimized pH was 7.4.

The response of the resultant ratiometric fluorescence probes toward different concentrations of Hg²⁺ has been studied and the corresponding fluorescence spectra were shown in Fig. 2. In the absence of Hg²⁺, two well-resolved emission peaks at 519 and 675 nm were observed under a single excitation at 365 nm, which can be attributed to the emission of FITC in the core and CdTe/CdS QDs on the surface of the silica nanoparticles, respectively. It was noted that the fluorescence intensity at 675 nm was highly sensitive to Hg²⁺ and decreased as the concentration of Hg²⁺ increased from 0 to 42 μM (Fig. 2A). The green fluorescence of FITC at 519 nm was also found decreased with the increasing of the Hg²⁺ concentration, but the extent of decrease was much less than that of the red fluorescence. As shown in Fig. S6, there is a little spectral overlap between between the emission spectrum of CdTe/CdS QDs and the absorption spectrum of FITC-doped silica core, which indicated that a slight fluorescence resonance energy transfer (FRET) from QDs to FITC-doped silica might occur. Therefore, the decrease of the emission at 519 nm might mainly attribute to the decrease of the FRET, which resulted from the reduction of the fluorescence intensity of QDs upon addition of Hg²⁺. Under optimal conditions, the fluorescence intensity ratio increased linearly with the concentration of Hg²⁺ ranging from 1.0×10^{-6} to 9.0×10^{-6} M (Fig. 2B, inset) and the limit of detection for Hg²⁺ was 3.4×10^{-7} M based on the definition of three times the deviation of the blank signal (3σ). More importantly, the slight decrease of the fluorescence from CdTe/CdS QDs could result in distinguishable color changes under a UV lamp (Fig. 2C), confirming that the validity of the FITC doped silica core as an internal calibration and the visual detection of Hg²⁺ by the naked eye is feasible. Moreover, the advantages of the ratiometric probe for visual detection of Hg²⁺ is verified by the comparison with the single fluorescence quenching experiment, in which only a pure red NAC capped CdTe/CdS QD probe is employed for the detection of Hg²⁺ (Fig. S7). Unlike the ratiometric probe, the color changes of the single fluorescence quenching of the red NAC capped CdTe/CdS QDs upon the addition of Hg²⁺ are hard to observe (Fig. S8). The comparison clearly shows that the ratiometric fluorescence probe possesses higher sensitivity and reliability than a single fluorescence quenching probe for visual detection.

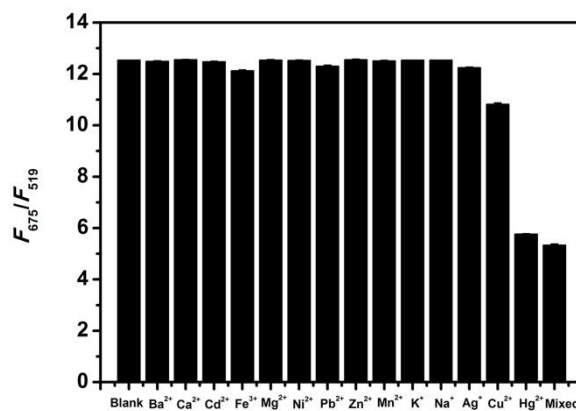


Fig. 3 Fluorescence intensity ratio of F_{675}/F_{519} in the presence of different concentrations of various metal ions (Hg²⁺: 9 μM, other: 20 μM). F_{675} and F_{519} correspond to the fluorescence intensity of the ratiometric probe at the emission wavelength of 675 and 519 nm respectively in the absence and presence of various metallic ions. The final concentration of the ratiometric probe was 0.25 mg mL⁻¹.

To evaluate the selectivity of the nanoprobe to Hg²⁺, we measured the fluorescence intensity ratio (F_{675}/F_{519}) in the presence of Hg²⁺ and other representative metallic ions Ba²⁺, Ca²⁺, Cd²⁺, Fe³⁺, Mg²⁺, Ni²⁺, Pb²⁺, Zn²⁺, Mn²⁺, K⁺, Na⁺, Ag⁺, and Cu²⁺ under the same conditions. As displayed in Fig. 3, in the presence of other ions, the fluorescence intensity ratio did not show significant change compared with the dual-emission nanoparticles (blank), suggesting the good selectivity of the ratiometric fluorescence probe toward Hg²⁺ over other metal ions. Furthermore, the nanoprobe still demonstrated an excellent selectivity in the presence of all possible interference ions. The fluorescence quenching mechanism of Hg²⁺ in this case may be complex: both ion-binding and electron transfer can lead to the decrease of QD emission.¹² The red-shift from 675 to 685 nm in fluorescence spectra (Fig. 2A) is attributed to strong binding of Hg²⁺ onto the surface of NAC capped-CdTe/CdS QDs.¹⁸ On the other hand, like our previous work, the fast response of the QDs to Hg²⁺ (with 2 min, Fig. S9) revealed the selective fluorescence quenching could also arise from the stronger affinity of N atom (from NAC) to Hg²⁺ through fast electron transfer process than other metallic ions.¹⁷

Table 1 Direct determination of Hg²⁺ content in Hg²⁺-spiked tap water and lake water samples using the proposed ratiometric probe

Sample	Added Hg ²⁺ concentration (μM)	Found Hg ²⁺ concentration (μM)		Recovery	RSD (n=5)
		This method	CV-AFS ^a		
Tap water	2.0	2.08	1.97	104.0%	4.9%
	6.0	6.21	6.07	103.5%	2.3%
Lake water	2.0	2.13	2.06	106.5%	5.1%
	6.0	5.84	6.03	97.33%	3.4%

^aCold-vapour atomic fluorescence spectrometry

These initial results indicated that the dual-emission hybrid nanoparticles could be developed as an effective ratiometric fluorescence probe for the sensing of Hg²⁺. To further confirm its practicality in real samples, the ratiometric probe has been applied to

determine the concentration of Hg²⁺ in real water samples spiked with different amounts of Hg²⁺ in both tap water and lake water. As shown in Table 1, it can be seen that the estimated recoveries and RSD of the measurements were in the range of 97.33-106.5% and 2.3-5.1%, respectively, which were satisfactory for quantitative assays performed in real samples. Moreover, the proposed method analysis results were comparable with the results obtained by CV-AFS suggesting that the as-prepared ratiometric fluorescence probe was reliable and practical.

Conclusions

In summary, a ratiometric fluorescence probe for Hg²⁺ has been designed and fabricated by chemisorption numerous CdTe/CdS QDs upon the surfaces of the FITC-doped silica spheres. The nanoprobe takes advantage of the high stability of the dye-doped silica, the superior fluorescence properties of QDs as well as the specificity of NAC toward Hg²⁺. The ratiometric fluorescence probe provided an effective platform for rapid and reliable detection of Hg²⁺ in solutions on the basis of the measurement of both ratiometric fluorescence intensity and fluorescence color changes. Additionally, the ratiometric fluorescence probe has been successfully applied for the determination of spiked Hg²⁺ in real water samples.

Acknowledgements

We thanked Prof. C. Zhang, from Zhejiang University of Technology, Hangzhou, for the fluorescence experiments and gratefully acknowledge the financial support from National Natural Science Foundation of China (21405139), Zhejiang Provincial Natural Science Foundation of China (LY13E020009), Public Project of Zhejiang Province (2014C31152) and scientific research start-up funding of Zhejiang University of Technology (101010629).

Notes and references

^a College of Chemical Engineering, Zhejiang University of Technology, Hangzhou, 310014, PR China. E-mail: amchen@zjut.edu.cn; hjzjut@zjut.edu.cn

^b College of Materials Science and Engineering, Zhejiang University of Technology, Hangzhou, 310014, PR China.

Electronic Supplementary Information (ESI) available: [details of any supplementary information available should be included here]. See DOI: 10.1039/c000000x/

- 1 M. Valko, H. Morris and M. Cronin, *Curr. Med. Chem.*, 2005, **12**, 1161-1208.
- 2 M. Peng, Z.-A. Li, X. Hou and C. Zheng, *J. Anal. Atom. Spectrom.*, 2014, **29**, 367-373.
- 3 Z. Liu, Z. Zhu, H. Zheng and S. Hu, *Anal. Chem.*, 2012, **84**, 10170-10174.
- 4 X.-P. Yan, Z.-M. Ni and Q.-L. Guo, *Anal. Chim. Acta*, 1993, **272**, 105-114.
- 5 Y. Li, X.-P. Yan, L.-M. Dong, S.-W. Wang, Y. Jiang and D.-Q. Jiang, *J. Anal. Atom. Spectrom.*, 2005, **20**, 467-472.
- 6 Y. Li, Y. Jiang, X.-P. Yan and Z.-M. Ni, *Environ. Sci. Technol.*, 2002, **36**, 4886-4891.

- 7 L.-M. Dong, X.-P. Yan, Y. Li, Y. Jiang, S.-W. Wang and D.-Q. Jiang, *J. Chromatogr. A*, 2004, **1036**, 119-125.
- 8 X. Ding, L. Kong, J. Wang, F. Fang, D. Li and J. Liu, *ACS Appl. Mater. Interface.*, 2013, **5**, 7072-7078.
- 9 X. Chen, C. Han, H. Cheng, Y. Wang, J. Liu, Z. Xu and L. Hu, *J. Chromatogr. A*, 2013, **1314**, 86-93.
- 10 J. Nan and X.-P. Yan, *Chem. Commun.*, 2010, **46**, 4396-4398.
- 11 H. R. Rajabi, M. Roushani and M. Shamsipur, *J. Electroanal. Chem.*, 2013, **693**, 16-22.
- 12 Y.-S. Xia and C.-Q. Zhu, *Talanta*, 2008, **75**, 215-221.
- 13 J. Zhang, Y. Zhou, W. Hu, L. Zhang, Q. Huang and T. Ma, *Sensor. Actuat. B: Chem.*, 2013, **183**, 290-296.
- 14 C.-C. Huang, Z. Yang, K.-H. Lee and H.-T. Chang, *Angew. Chem. Int. Edit.*, 2007, **46**, 6824-6828.
- 15 C. Guo and J. Irudayaraj, *Anal. Chem.*, 2011, **83**, 2883-2889.
- 16 Y. Shen, Y. Zhang, X. Zhang, C. Zhang, L. Zhang, J. Jin, H. Li and S. Yao, *Anal. Methods*, 2014, **6**, 4797-4802.
- 17 J. Wang, N. Li, F. Shao and H. Han, *Sensor. Actuat. B: Chem.*, 2015, **207**, Part A, 74-82.
- 18 Z.-X. Cai, H. Yang, Y. Zhang and X.-P. Yan, *Anal. Chim. Acta*, 2006, **559**, 234-239.
- 19 X. Zhang, Y. Xiao and X. Qian, *Angew. Chem. Int. Edit.*, 2008, **47**, 8025-8029.
- 20 D. W. Domaille, L. Zeng and C. J. Chang, *J. Am. Chem. Soc.*, 2010, **132**, 1194-1195.
- 21 X. Cheng, Q. Li, J. Qin and Z. Li, *ACS Appl. Mater. Interface.*, 2010, **2**, 1066-1072.
- 22 Y. Jiang, H. Zhao, N. Zhu, Y. Lin, P. Yu and L. Mao, *Angew. Chem. Int. Edit.*, 2008, **47**, 8601-8604.
- 23 S. Han and Y. Chen, *Anal. Methods*, 2011, **3**, 557-559.
- 24 X. Cheng, Q. Li, C. Li, J. Qin and Z. Li, *Chem-A Eur. J.*, 2011, **17**, 7276-7281.
- 25 A. Burns, H. Ow and U. Wiesner, *Chem. Soc. Rev.*, 2006, **35**, 1028-1042.
- 26 K. Ai, B. Zhang and L. Lu, *Angew. Chem. Int. Edit.*, 2009, **48**, 304-308.
- 27 A. Guerrero-Martínez, J. Pérez-Juste and L. M. Liz-Marzán, *Adv. Mater.*, 2010, **22**, 1182-1195.
- 28 C. H. Zong, K. L. Ai, G. Zhang, H. W. Li and L. H. Lu, *Anal. Chem.*, 2011, **83**, 3126-3132.
- 29 K. Zhang, H. Zhou, Q. Mei, S. Wang, G. Guan, R. Liu, J. Zhang and Z. Zhang, *J. Am. Chem. Soc.*, 2011, **133**, 8424-8427.
- 30 J. L. Yao, K. Zhang, H. J. Zhu, F. Ma, M. T. Sun, H. Yu, J. Sun and S. H. Wang, *Anal. Chem.*, 2013, **85**, 6461-6468.
- 31 Y. Q. Wang, T. Zhao, X. W. He, W. Y. Li and Y. K. Zhang, *Biosens. Bioelectron.*, 2014, **51**, 40-46.
- 32 X. J. Liu, N. Zhang, T. Bing and D. H. Shangguan, *Anal. Chem.*, 2014, **86**, 2289-2296.
- 33 X. Wang, O. Ramstrom and M. D. Yan, *Chem. Commun.*, 2011, **47**, 4261-4263.
- 34 H. Dong, F. Yan, H. Ji, D. K. Y. Wong and H. Ju, *Adv. Funct. Mater.*, 2010, **20**, 1173-1179.